*Assiut University Center for Environmental Studies-Egypt*

**The 9th Int. Conf. for Develop. and the Env . in the Arab world, April, 15-17, 2018**

# UTILIZATION OF THE CLAYSTONES FROM THE QUSEIR AREA, RED SEA, EGYPT, IN THE SYNTHESIS OF ZEOLITES AND THEIR USES FOR WATER REMEDIATION

**Fatma Dardir**

**Geology Department, Faculty of Science, Assiut University, Egypt**

## ABSTRACT

**This article deals principally with the evaluation of the Late Cretaceous – Early Paleogene claystones accumulated under different environmental regimes in the synthesis of zeolite minerals. The studied claystones were accumulated under fluviatile, tide and open marine conditions. XRD of the bulk claystone samples collected from the different environmental settings indicated that these claystones are composed of quartz, smectite, kaolinite and calcite. Hydrothermal treatment of the raw material with NaOH at 80°C and 160°C led to the formation of faujasite and sodalite respectively which were verified by XRD, SEM, FT – IR and nitrogen sorption methods. Faujasite and sodalite have revealed enormous removal capacity of heavy metals from the prepared slandered solution polluted by Co, Pb, Cd, Zn and Cu and organic matter (methylene blue dye). Generally, their propensity for the removal of heavy metals is higher than the organic matter. The former reaches up to 99.9% whereas, the second one reaches up to 75.5%. Moreover, there is no significant variation in the removal capacity between faujasite and sodalite.**

## INTRODUCTION

**Water pollution (heavy metals and organic matter) is one of the most important environmental issues in the developing countries which represents a real challenge facing modern society leads to ecological imblance and health hazard. Discharge of heavy metals via different sources (mining activites, industries and irrigation) especially in the areas with limited water sources as in our case is quite normal. The heavy metals pollution of drinking water with Co, Pb, Zn, Cd and Cu can lead to serious human health hazards through the food chain which can harm the whole biological environment (Hafiza *et al.*, 2015).**

**The admissible limits of the heavy metals concentarion in the drinking water show a slight variation between World Health Organization (WHO), the U.S. Environmental Protection Agency (USEPA) and the European Union (EU) (Table 1). Increasing the metal ion concentrations above the recommended levels convert such ions into a toxic element in the body (Manohar *et al.*, 2006; Sen & Gomez, 2011). In the recent years, porous materials attracted wide attention as efficient adsorbent materials for water contaminants as**

**they are characterized by high specific surface area, large pore volume, facile mass transportation, active adsorption sites and high cation exchange capacity (Rhaiti *et al.*, 2012; Chowdhury & Naskar, 2016).**

**Table 1: Drinking water guideline standard concentration for heavy metals set by the World Health Organization (WHO), the U.S. Environmental Protection Agency (USEPA) and the European Union (EU)**

| Contaminant | Unit | Guideline value (WHO) | Environmental Protection Agency (USEPA) | European Union (EU) |
|---|---|---|---|---|
| Pb | µg/l | 10 | 15 | 10 |
| Zn | | 3000 | 5000 | 5000 |
| Cd | | 3 | 5 | 5 |
| Cu | | 2000 | 1300 | 2000 |
| Co | | 50 | 100 | —— |

—— Not determined

**Most of the previous studies carried out in Egypt were addressed to use the kaolin of Sinai as a raw material for the synthesis of zeolites. Synthesis of zeolites using different claystone varieties that were accumulated under different environmental settings at the Quseir area (Fig.1) is the goal of the present study. In this context, it is worthy to mention here that the study area received seasonally a plenty of rainfall and torrents (550 $m^3$/ year) in addition to mining activities, therefore the groundwater is expected to be polluted. Accordingly, this area represents a real chance to check the capabilities of the prepared synthetic materials for the removal of pollutants (heavy metals and organic matter).**

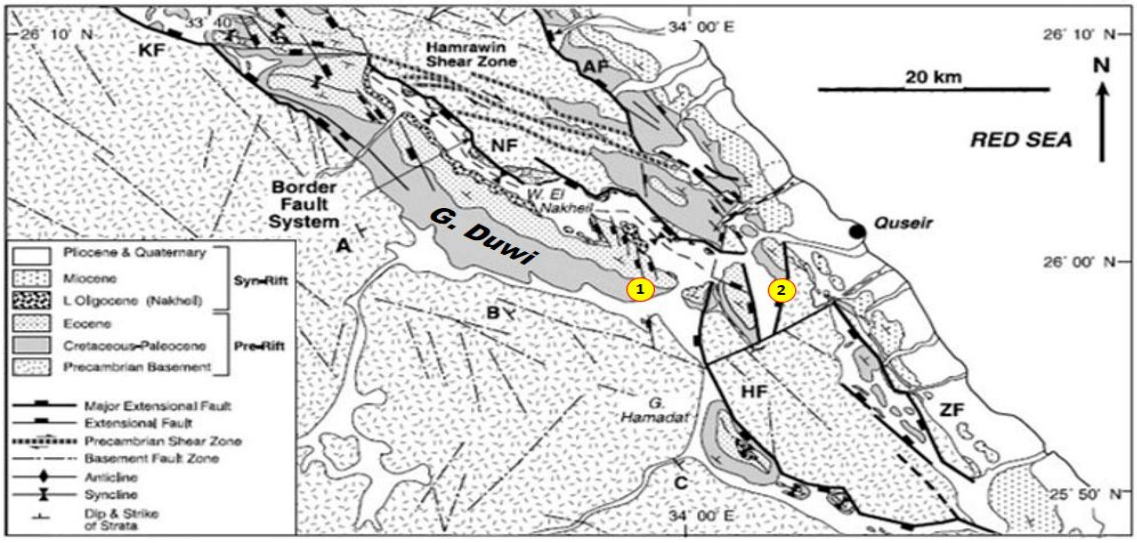


**Fig.1. Geological map of the study area (After Khalil, S. M and McClay, K. R ,2002)**
**(1 Duwi , 2 Zug El- Bohar)**

# 1. GEOLOGICAL BACKGROUND

**The Late Cretaceous – Early Paleogene sedimentary package exposed at the Quseir area is represented by siliciclastics, phosphorites and carbonates (Fig.2). This sequence starts at the base with the Nubia Sandstone, followed upwards by the Quseir Formation, Duwi Formation, Dakhla Formation, Esna Formation and finally capped with the Thebes Formation (Said, 1990). Such succession could be subdivided into distinctive sixteen sedimentary facies ($F_1$ – $F_{16}$) and was accumulated under different environmental regimes which can be subdivided, in a broad sense, into: fluviatile sediments ($F_1$&$F_2$), tidal flat sediments ($F_3$ – $F_6$) and open marine sediments ($F_9$ – $F_{16}$). Three field visits to the Quseir area, in particular, G. Duwi and Zug El- Bohar were successfully done to achieve detailed field studies and to collect the samples required for the synthesis of zeolites. Detailed description of the sedimentary facies documenting all the characteristics of lithology, geometry of sedimentary structures which can aid in determining the sedimentary processes that dominated during the time of deposition and thus the interpretation of sedimentary environments is included in the M.Sc. thesis of Dardir (in preparation). The different lithologies within each rock unit forming a rhythmic pattern of cycles, finning or coarsening upwards (Fig.2).**

# 2. HISTORICAL BACKGROUND

**The term zeolite was extensively introduced in the scientific articles and theses since the work of the Cronstedt (1756). Zeolites are microporous crystalline hydrated aluminosilicates characterized by a three – dimensional network of tetrahedral (Si, Al) $O_4$ that form a system of interconnected pores (Ltaief *et al*., 2015). Synthesis of zeolites can be prepared from a number of source materials. Clay mineral is one of the most often used for this purpose (Novembre *et al*., 2004). The first laboratory synthesis of zeolites dated back to Deville (1862). He synthesized Levynite by heating potassium silicate and sodium aluminate in a glass ampoule. Barrer (1938) successfully synthesized Chabazite and Mordenite, leading to inspiring periods of zeolite synthesis in the search of new approaches for the separation and purification of air (Flanigen, 2001). Until now about 150 synthetic zeolites and more than 40 natural mineral species were recorded.**

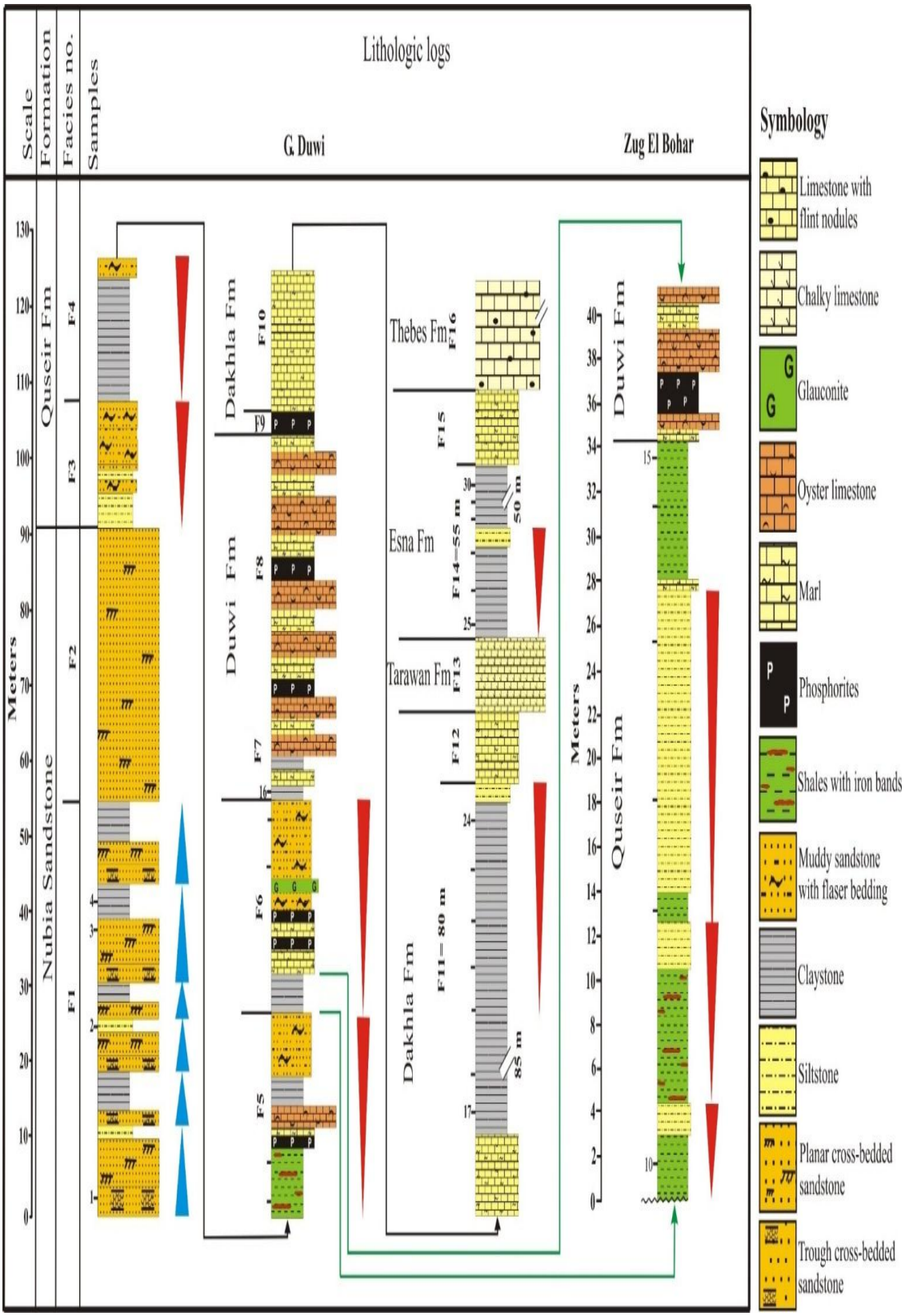


**Fig.2. Sedimentary facies evolution of G. Duwi and Zug El – Bohar localities, Quseir area**

## 4. MATERIALS AND METHODS

**Fourteen claystone samples selected from the collected ones were used in the synthesis of zeolites, one sample belonging to fluviatile sediments (Nubia Sandstone), eight samples belonging to tidal flat sediments (Quseir Formation) and five samples picked out from the open - marine system (Dakhla and Esna formations). These samples were investigated using XRD to explore their mineralogical composition.**

**XRD has revealed that the claystone samples belonging to the Nubia Sandstone are composed of kaolinite and quartz (Fig.3). The claystone samples of the Quseir Formation have demonstrated the existence of smectite, Kaolinite and quartz (Fig.4). Examination of Dakhla and Esna formations samples show that smectite, kaolinite, quartz and calcite are the encountered minerals composing the scanned claystones (Fig.5).**

**The major constituents of the utilized claystones were analyzed by XRF and the results are given in Table 2. The molar Si/Al ratio was calculated to shed light on their importance for the evaluation of the product zeolite types. The marine claystones are usually enriched in heavy metals compared with the fresh ones due to their variable sources (internal and external) during their deposition. Therefore, someone can thinking on the release of some heavy metals from the raw materials used in experimental work. To be sure about that 0.025g of the raw material was added to 50ml. distilled water and stirred for 1 h. The concentration of Cd, Co, Cu, Pb and Zn in the solution were measured using Inductively Coupled Plasma Emission Spectrometer (ICP 6200), at Assiut University. The concentration of Cd, Co, Cu, Pb and Zn were found to be less than 1 ppm, which confirmed that nothing could be add from the utilization of the raw materials to the experimental work.**

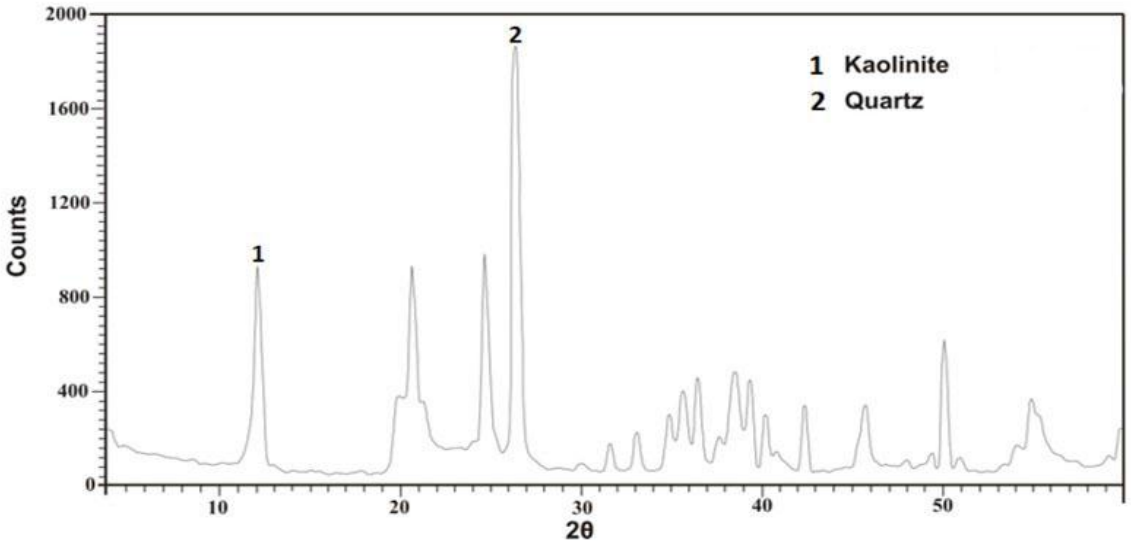


**Fig.3. XRD of bulk claystone, sample 3, $F_1$, Nubia Sandstone, G. Duwi**

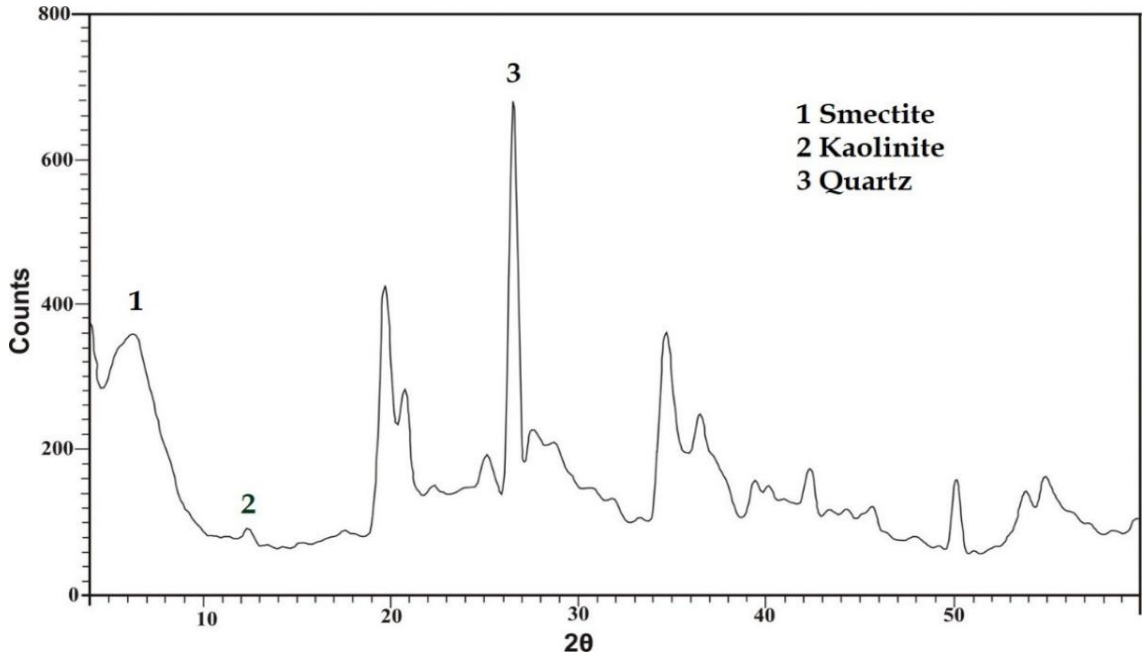


**Fig.4. XRD of bulk claystone, sample 9, $F_{5-6}$, Quseir Formation, G. Duwi**

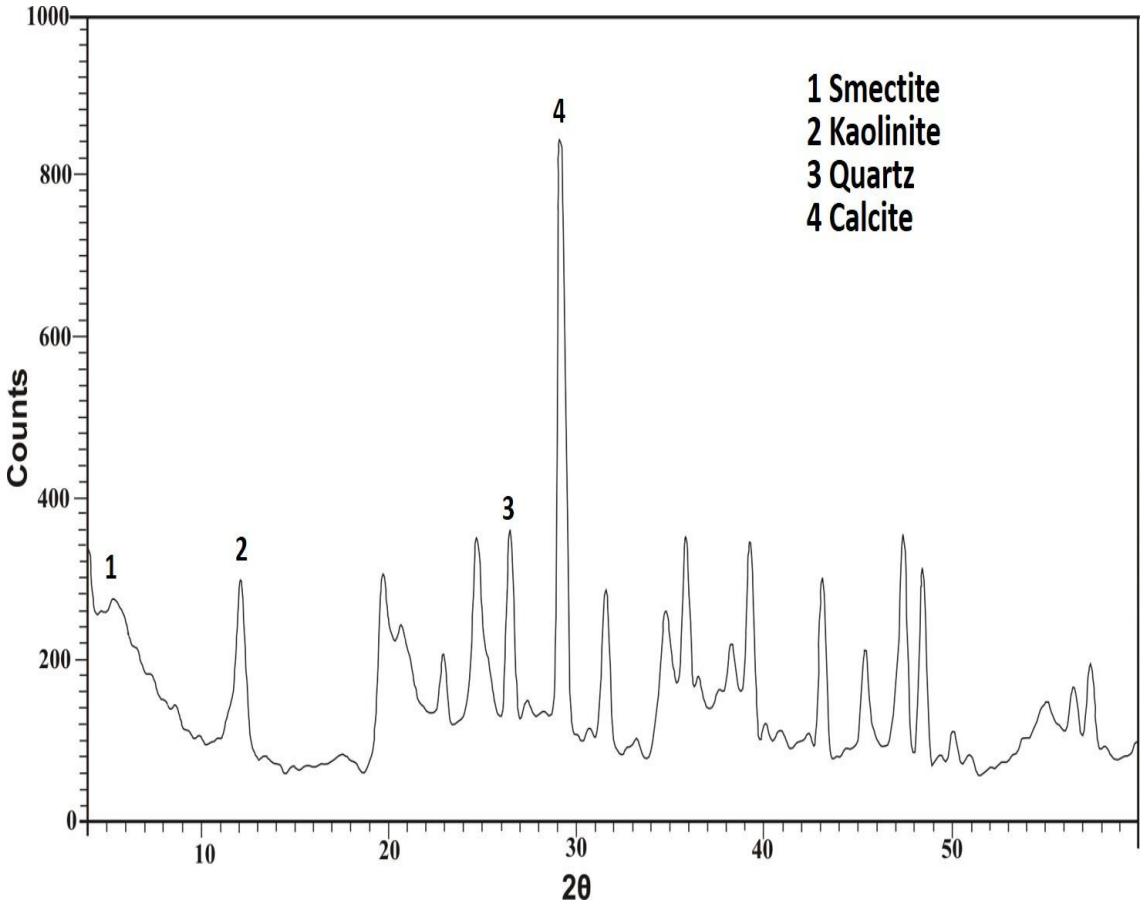


**Fig.5. XRD of bulk claystone, sample 18, $F_{10}$-$F_{11}$, Dakhla Formation, G. Duwi**

**Table 2: Results of chemical analysis**

| Samples/oxides | | | $SiO_2$ | $TiO_2$ | $Al_2O_3$ | $Fe_2O_3$ | MnO | MgO | CaO | $Na_2O$ | $K_2O$ | $P_2O_5$ | $H_2O^+$ | TOTAL | Si/Al Molar ratio |
|---|---|---|---|---|---|---|---|---|---|---|---|---|---|---|---|
| Quseir Fm. | *Tidal flat sediments* | 6 | 48.569 | 1.187 | 17.39 | 14.708 | 0.023 | 3.351 | 7.588 | 0.632 | 2.071 | 3.858 | 0.446 | 99.826 | 2.37 |
| | | 7 | 63.618 | 1.311 | 19.01 | 5.812 | 0.008 | 3.373 | 2.834 | 1.226 | 1.935 | 0.058 | 0.474 | 99.659 | 2.85 |
| | | 10 | 66.83 | 1.511 | 19.292 | 5.737 | 0.011 | 3.029 | 0.005 | 0.929 | 1.466 | 0.072 | 0.457 | 99.339 | 2.95 |
| | | 12 | 68.608 | 0.802 | 11.334 | 6.54 | 0.027 | 3.42 | 3.476 | 0.622 | 1.781 | 2.485 | 0.387 | 99.481 | 5.15 |
| Dakhla Fm. | *Open marine sediments* | 17 | 44.461 | 0.717 | 21.723 | 5.93 | 0.02 | 2.003 | 22.046 | 0.915 | 1.082 | 0.611 | 1.013 | 100.522 | 1.74 |
| | | 19 | 45.411 | 0.88 | 25.992 | 8.386 | 0.123 | 1.98 | 14.778 | 0.805 | 0.862 | 0.358 | 0.89 | 100.466 | 1.49 |
| | | 24 | 38.314 | 0.642 | 17.988 | 6.015 | 0.019 | 2.59 | 31.334 | 0.671 | 0.306 | 0.94 | 1.251 | 100.069 | 1.81 |
| Esna Fm. | *Open marine sediments* | 26 | 50.397 | 0.725 | 19.948 | 6.562 | 0.015 | 3.208 | 15.344 | 1.807 | 1.133 | 0.421 | 0.723 | 100.283 | 2.15 |
| | | 27 | 25.704 | 0.353 | 9.947 | 3.05 | 0.012 | 1.893 | 55.694 | 0.383 | 0.062 | 1.174 | 1.169 | 99.441 | 2.20 |
| | | 29 | 35.05 | 0.59 | 17.568 | 6.933 | 0.02 | 2.188 | 34.378 | 1.163 | 0.919 | 0.405 | 1.153 | 100.366 | 1.70 |
| | | 30 | 47.482 | 0.522 | 14.492 | 4.336 | 0.021 | 4.768 | 25.039 | 1.384 | 0.894 | 0.219 | 1.164 | 100.321 | 2.79 |

**For the location of the analyzed samples see Figure 2**

# 5. EXPERIMENTAL

## 5.1. Optimal synthesis of zeolites

**Synthesis of zeolites was achieved following Ríos et al (2009) where the powdered samples (< 250 mesh) were sieved to remove the oversize particles. The fraction (< 62 mm) was treated by $H_2O_2$ and diluted HCl to remove the organic matter and carbonates respectively. The prepared samples were washed by distilled water and dried at 100 °C and then heated at 650 °C for 4h. Subsequently, 10 g from each sample added to 12 g NaOH and heated at 650 °C for 4h. Additionally, 8.8 g from each one added to 43ml of distilled water on teflon crucible and stirred for 2h and leaved it overnight. Teflons were placed on the oven for 48h at 80 °C, 100 °C and 160 °C. Finally, the samples filtrated, washed with distilled water to pH lower than 11 and dried at 60 °C. The prepared synthetic materials were characterized in terms of XRD, SEM, FT - IR and Surface area properties at Assiut University.**

# 6. CHARACTERIZATION OF ZEOLITES

## 6.1. X-ray diffraction (XRD)

**The synthesized materials were scanned between 4-60° 2θ using XRD equipment. The obtained results has revealed a marked variation on the XRD lines between the treated samples at 80 and 160° C. The treated material at 80° has illustrated a well prominent intense main peak at 6.2 2θ (Fig.6). The secondary peaks occur at 15°.16 2θ, 18°.64 2θ, 20°.30 2θ and 23°.58 2θ. These peaks specifying faujasite mineral. In contrast, the samples treated at 160° have revealed distinctively different XRD lines. Where, the main peak was encountered at 24°.65 2θ. 14°.16 2θ, 35°.13 2θ and 31°.99 2θ are the secondary peaks characterizing the second materials. The resultant peaks match well with the sodalite mineral (Fig.7). The crystallite size of both faujasite and sodalite minerals were calculated applying Scherrer's formula; D = 0.9λ / W Cosθ; where W is in radians, θ is the Bragg's angle, λ is the X-ray wavelength (CuKα = 0.15405 nm). 21.85 nm and 18.14 nm are the crystallite size of faujasite and sodalite respectively (Table 3).**

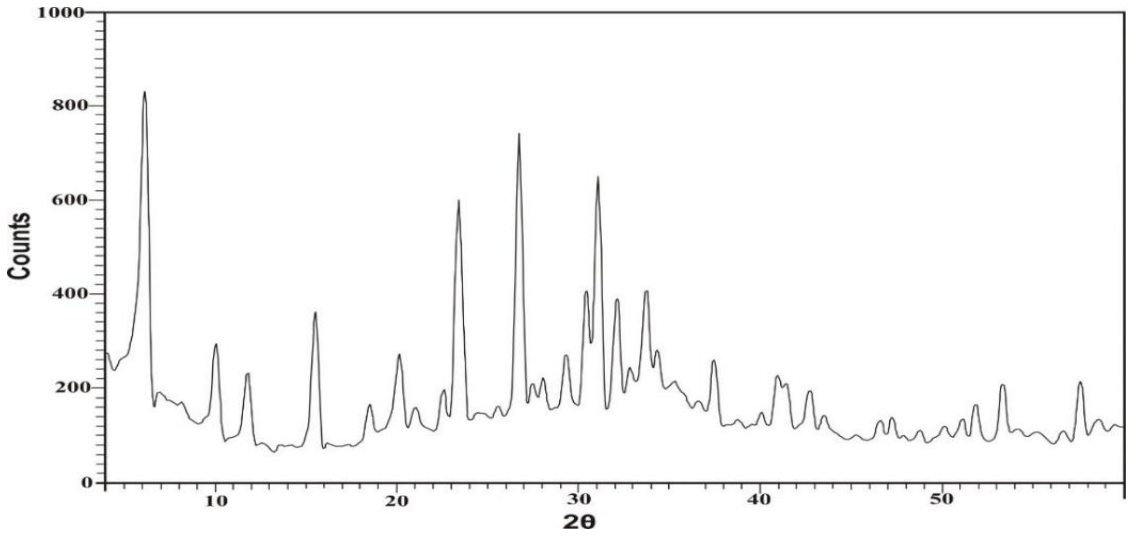


**Fig.6. XRD of the synthesized faujasite, sample 6, $F_5$-$F_6$, Quseir Formation, G. Duwi**

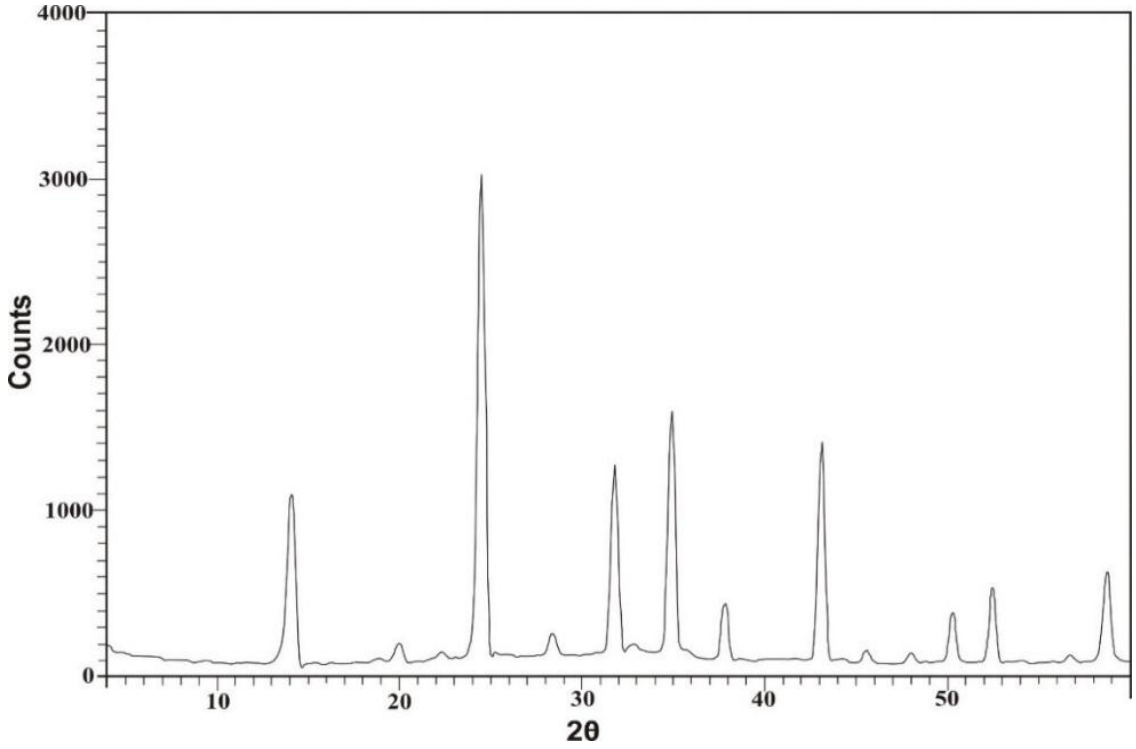


**Fig.7. XRD of the synthesized sodalite, sample 18, $F_{10}$-$F_{11}$, Dakhla Formation, G. Duwi**

**Table 3. Average crystallite size of the synthesized zeolite minerals based on XRD results**

| *Zeolite mineral* | *Crystallite size* |
|---|---|
| *Faujasite* | *21.85 nm* |
| *Sodalite* | *18.14 nm* |

## 6.2. Scanning Electron Microscope (SEM)

**To study the morphology of the synthesized zeolites, small part of the prepared materials were mounted on the SEM holders and coated with evaporated thin carbon films, examined and photographed using the Scanning Electron Microscope at Assiut University. Well crystallized octahedral shape (Fig.8 A) and thread - ball like and armadillo – like particles (Fig.8 B) were encountered in the examined samples. The former one characterizes faujasite mineral (Ríos *et al.*, 2009), whereas, the second one characterizes sodalite mineral (Hums, 2017).**

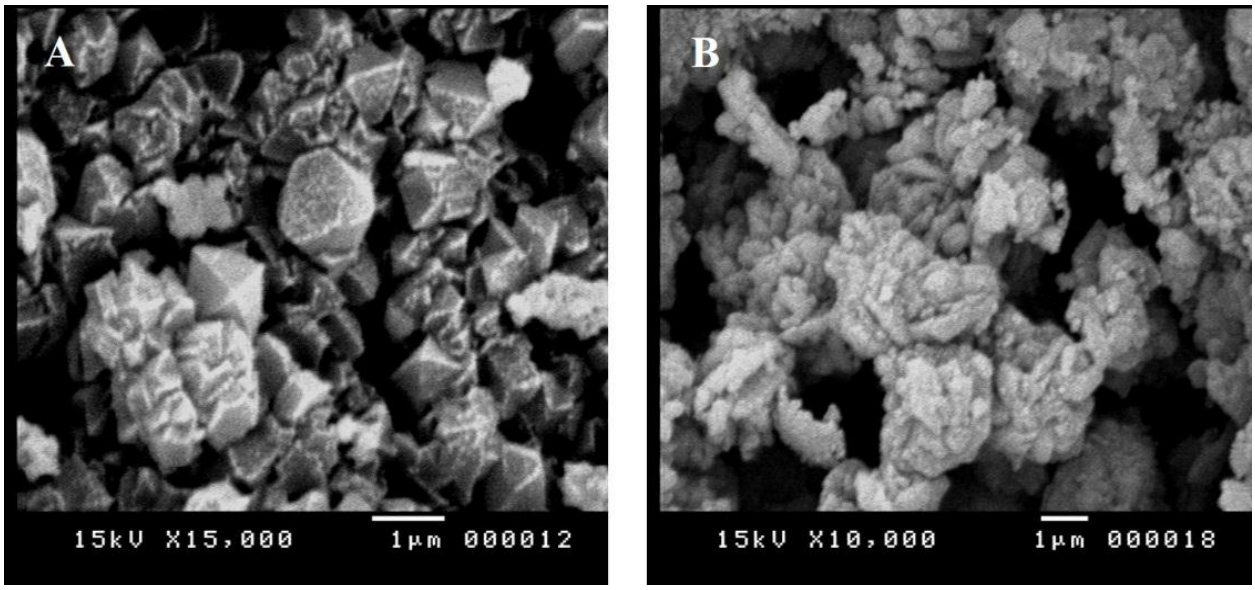


**Fig.8.** **SEM of octahedral faujasite (A) and thread - ball like and armadillo – like particles of sodalite (B), $F_{10}$ - $F_{11}$, Dakhla Formation, G. Duwi**

## 6.3. Fourier – transform infrared (FT-IR) spectroscopy

**The synthesized samples were subjected to FT – IR examinations with a Nicolar spectrophotometer (model 6700) FT-IR equipped with data station. Dried samples of about 20 mg were mixed with 100 mg of dry spectral grade KBr and pressed into disk under hydraulic pressure. FT – IR of the first synthesized zeolites indicates well prominent absorptions at 459, 500, 668, 748, 977, 1655 and 3466 $cm^{-1}$ (Fig.9 A). These data fits well with the results of faujasite recorded by Thuadaija and Nuntiya (2012). The 979 $cm^{-1}$ band is due to the Si-O-Al antisymmetric stretching vibration mode of T-O bands (where T = Si or Al) (Joshi et al, 2003 and Mozgawa, 2001). FT – IR of the second synthesized material shows well marked bands at 463, 665, 736, 977, 1653 and 3502 $cm^{-1}$ (Fig.9 B). These results coincide with those reported for sodalite (Henderson & Taylor, 1977).**

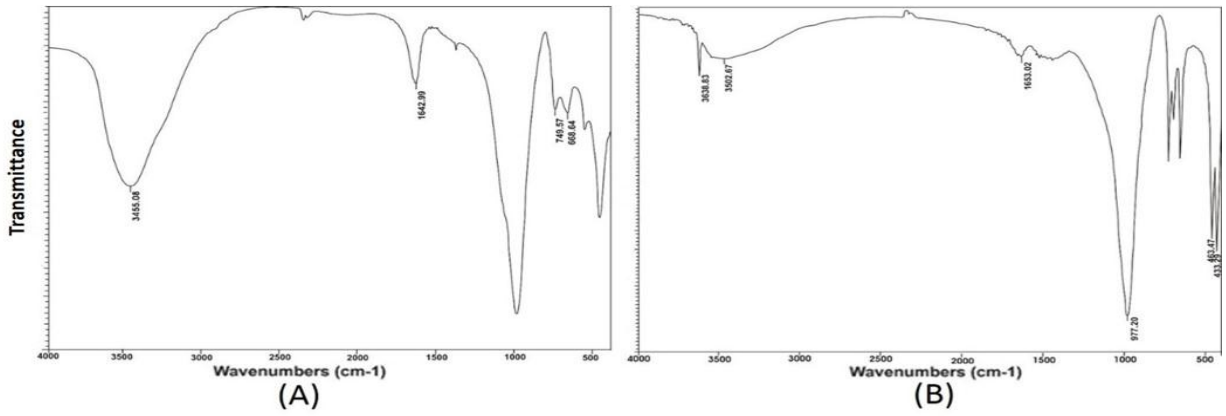


**Fig.9.** **FT- IR of synthesized faujasite (A) and sodalite (B)**

## 6.4. Surface area properties

**Nitrogen adsorption – desorption isotherms were measured using liquid nitrogen at -196°C by the Quantachrom Instrument Corporation, USA (Model Nova 3200). Test samples were thoroughly out gassed for 2h at 250 °C. The porosity of the prepared synthetic materials were determined from the desorption curve using Nova enhanced data reduction software (Version 2.13). The obtained results have revealed that a well marks difference between faujasite and sodalite was found. The former has surface area about 401 $m^2$/g, whereas the second reaches up to 70 $m^2$/g (Table 4). Ltaif *et al* (2015) mentioned that the surface area of faujasite synthesized from clays is 360 $m^2$/g. Golbad (2016) studied the sodalite synthesized from fly ash and reported that the surface area of it is 40 $m^2$/g. The average pore diameter of faujasite was found to be less than sodalite (Table 4).**

**Table 4. Results of surface area of faujasite and sodalite**

| *Sample* | *$S_{BET}$ ($m^2$/g)* | *Total pore volume (CC/g) × $10^{-2}$* | *Average pore diameter (Å)* |
|---|---|---|---|
| *Faujasite* | *401.9* | *41.6* | *41.4* |
| *Sodalite* | *70.6* | *15.3* | *86.8* |

## 6.5. Preparation of contaminated water

**To prepare the contaminated water, standard solutions (10 mg/l, 20 mg/l, 30 mg/l, 40 mg/l, 50 mg/l, 60 mg/l, 80 mg/l, 100 mg/l) of Copper ($Cu^{2+}$), lead ($Pb^{2+}$), Zinc ($Zn^{2+}$), Cadmium ($Cd^{2+}$) and Cobalt ($Co^{2+}$) were prepared and mixed with deionized water in 1 L glass container. In addition, standard solutions (10 mg/l, 20 mg/l, 40 mg/l, 60 mg/l,80 mg/l,100 mg/l) of methylene blue dye were also prepared. To ensure that the contaminants remained solutions, the mixed solution was continuously stirred. The pH of the contaminated water was adjusted to a value of 4 using NaOH and $HNO_3$.**

# 7. REMOVAL OF WATER POLLUTANTS

## 7.1. Removal of heavy metals and organic matter (methylene blue dye)

**The uptake of Zn, Co, Cu, Cd and Pb and methylene blue dye was studied by using faujasite and sodalite in terms of contact time, adsorbent dosage, pH and initial concentration.**

### 7.1.1. Effect of contact time

**Two stages of heavy metals adsorption by faujasite and sodalite were observed (Fig.10 A& B). The first stage reflects rapid and sharp increases of uptake with increasing contact time followed by the second one until the reaction reaches the equilibrium stage. Such behavior may related to the decreases of the number of the adsorption active sites due to their saturation with the pollutant ions with time (Seliem *et al.,* 2016; Shaban *et al.,* 2017). The obtained results have revealed that the removal percentage of the studied metal ions by the synthesized materials follows the order:**

$$Pb^{2+} > Cd^{2+} > Cu^{2+} > Co^{2+} > Zn^{2+}$$

**This order of removal is consistent with increasing the ionic radius of the metal ions $Pb^{2+}$ (1.19Å), $Cd^{2+}$ (0.95Å) and $Cu^{2+}$ (0.73 Å). The similarity in the ionic radius of Co (0.70Å) and $Zn^{2+}$ (0.74 Å) shows no perfect arrangement. The same behavior of adsorption was observed using the polluted water with organic matter (methylene blue dye) (Fig.10 C).**

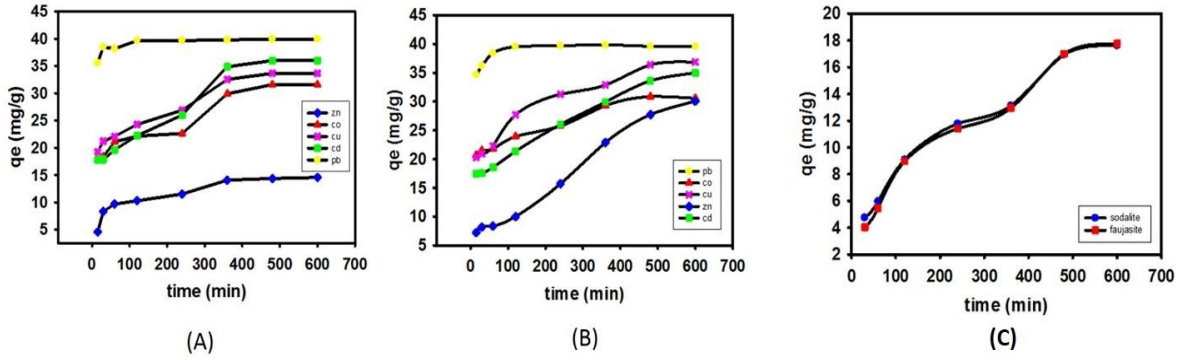


**Fig.10. Removal of heavy metals using synthesized faujasite (A) and sodalite (B) and methylene blue dye (C) from the polluted water as a function of contact time ($q_e$ = the amount of adsorbed heavy metals or dye)**

## 7.1.2. Effect of adsorbent dosage

**The dependence order of $Pb^{2+} > Cd^{2+} > Cu^{2+} > Co^{2+} > Zn^{2+}$ metal ions on the adsorption capacity was studied at different dosage of faujasite and sodalite (Fig.11 A& B). The adsorption of heavy metals increases with increasing adsorbent dosage which reached to the maximum removal percentage (more than 99%) by using faujasite and (more than 99%) for ($Pb^{2+}$, $Cd^{2+}$ and $Cu^{2+}$) by using sodalite. Less adsorption of $Co^{2+}$ and $Zn^{2+}$ by sodalite (about 80%) was noticed.**

**The removal of methylene blue dye using the synthesized faujasite and sodalite increases as the dose increases to 0.2 g which reached to 75% by using faujasite and 46% by using sodalite (Fig.11 C). Furthermore, a marked decline in the adsorption efficiency was noticed which may be related to the effect of zeolites on the pH value of the solution (cf. Polatoglu, 2005; Abudaia *et al.*, 2013).**

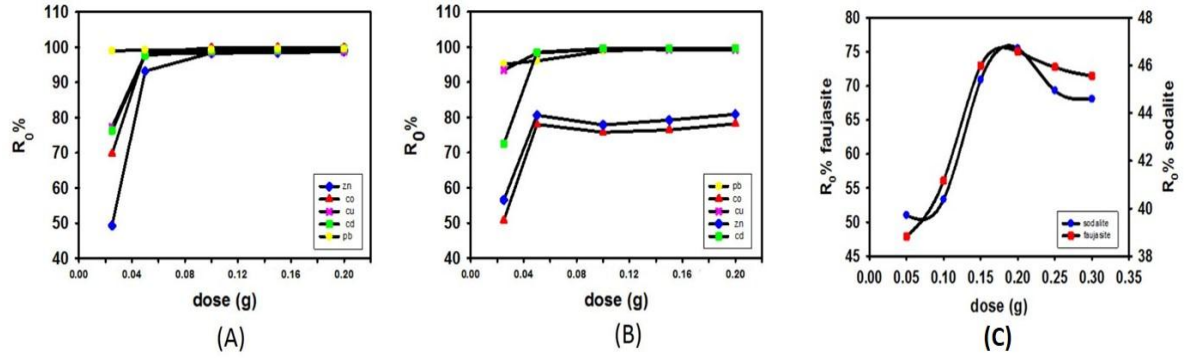


**Fig.11. Removal of heavy metals using synthesized faujasite (A) and sodalite (B) and methylene blue dye (C) from the polluted water as a function of adsorbent dosage ($R_0$ = adsorption percentage of heavy metals)**

## 7.1.3. Effect of pH

**The effect of pH on the removal percentage of $Zn^{2+}$, $Co^{2+}$, $Cu^{2+}$, $Cd^{2+}$ and $Pb^{2+}$ was studied using the synthesized faujasite and sodalite between appropriate pH values. The obtained results are illustrated in Figure 12 A& B. The optimum pH value required for the maximum removal was found to be around 5 for faujasite and 7 for sodalite. Also, the optimum pH value required for the complete of methylene blue dye was found to be around 7 by using faujasite and sodalite (Fig.12 C).**

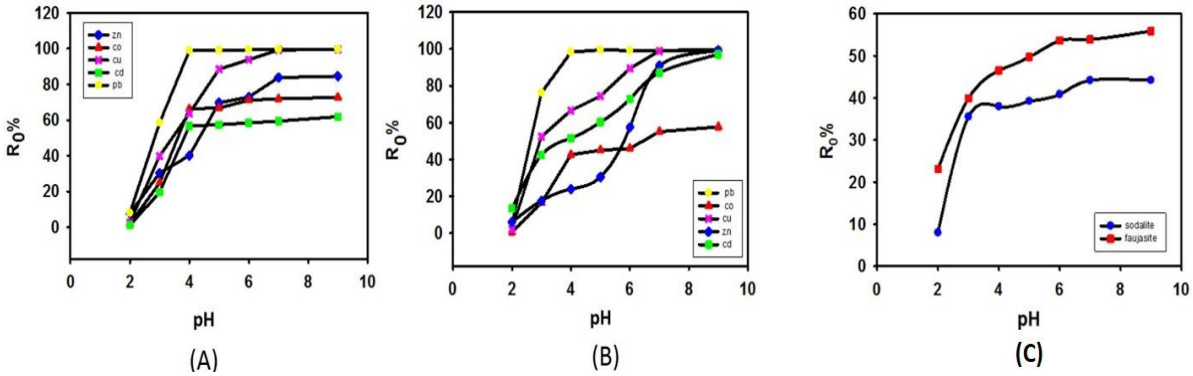


**Fig.12. Removal of heavy metals using synthesized faujasite (A) and sodalite (B) and methylene blue dye (C) from the polluted water as a function of pH**

## 7.1.4. Equilibrium studies

## 7.1.4.1. Effect of initial concentration

**The relationship between adsorption of the dissolved heavy metal ions with different initial concentration by using faujasite and sodalite are illustrated in Figure 13 A & B. The adsorption curves of heavy metal ions show that the adsorption capacity increases with increasing initial concentration until reached to the optimum conditions which after that the curves appear to be constant or slightly increased. The same behavior with methylene blue dye was also observed (Fig.13 C).**

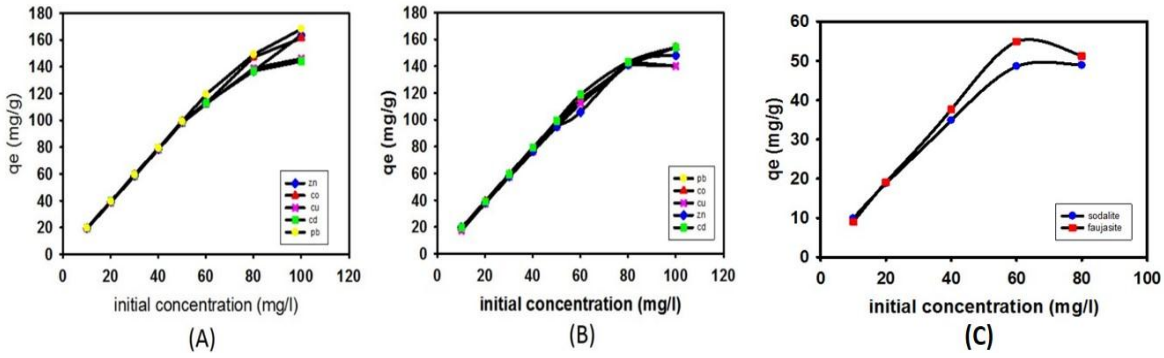


**Fig.13. Removal of heavy metals using synthesized faujasite (A) and sodalite (B) and methylene blue dye (C) from the polluted water as a function of initial concentration**
**($q_e$ = uptake capacity per unit mass at equilibrium mg/g)**

## 7.1.4.2. Isothermal studies

**Two isothermal models were applied herein to study the behavior of heavy metals and organic matter (methylene blue dye) using faujasite and sodalite. The first model is Langmuir isothermal model which was used to describe the adsorption system occurring in monolayer and homogeneous active adsorption sites (cf. Seliem *et al.*, 2016). Moreover, the adsorption process occurs without interaction between the adsorbed molecules (Allen *et al.*, 2003). The linear form of Langmuir was represented by Eq (1):**

$$\frac{Ce}{q_e} = \frac{1}{bq_{max}} + \frac{Ce}{q_{max}} \qquad (1)$$

**Where Ce is the final concentration of dissolved heavy metal ions in the solution after the adsorption process (mg/l), $q_e$ is the uptake capacity per unit mass at equilibrium (mg/g), $q_{max}$ is the amount of adsorbate per unit mass of adsorbent at complete monolayer coverage (m mol/g), and b is the Langmuir constant (L/mg). Plotting Ce/qe versus Ce by using faujasite and sodalite is shown in Figure 14. The obtained data illustrate very good fitting (correlation coefficient more than 0.9) which show that the adsorption of heavy metals and methylene blue dye occurs in monolayer form through a specific homogenous active of adsorption sites in faujasite and sodalite. The parameters of this model were calculated based on the slope and intercept and listed in Table 5. The calculated maximum adsorption capacity ($q_{max,cal}$) by using faujasite are 166.6 mg/g, 163.93 mg/g, 149.25 mg/g, 147.05 mg/g, 169.49 mg/g and 55.63 mg/g for the uptake of $Zn^{2+}$, $Co^{2+}$, $Cu^{2+}$, $Cd^{2+}$, $Pb^{2+}$ and methylene blue dye respectively. By using sodalite the calculated maximum adsorption capacity are 149.25 mg/g, 156.25 mg/g, 144.29 mg/g, 156.25 mg/g, 144.92 mg/g and 52.63 mg/g for the uptake of $Zn^{2+}$, $Co^{2+}$, $Cu^{2+}$, $Cd^{2+}$, $Pb^{2+}$ and methylene blue dye respectively.**

**The dimension less constant or the equilibrium parameters ($R_L$) is one of the most important parameters of Langmuir model, which reflects the nature of the adsorption process. $R_L$ values were calculated from equation (2) (Lian *et al.*, 2009):**

$$R_L = 1/(1+bC_0) \qquad (2)$$

**Where b is the Langmuir constant and $C_0$ is the initial concentration of heavy metals ions. The calculated $R_L$ values of $Zn^{2+}$, $Co^{2+}$, $Cu^{2+}$, $Cd^{2+}$, $Pb^{2+}$ and methylene blue dye are more than zero and less than one ($0 < R_L < 1$). Such result illustrates that the adsorption of heavy metals is favorable by using synthetic faujasite and sodalite (Table 5).**

**The second model is Freundlich model (Fig.15) which was used herein to describe the adsorption process occurring in multilayer (Bagherifam *et al.*, 2014). Freundlich isothermal model was represented by Eq (3):**

$$\text{Log } q_e = (1/n) \log C_e + \log K_f \qquad (3)$$

**Where $K_f$ and n are the Freundlich constant identified with adsorption capacity and intensity, respectively. Plotting log $q_e$ versus log $C_e$ reflects moderately fitting of $Zn^{2+}$, $Cd^{2+}$ and $Cu^{2+}$ ($0.8 > R^2 > 0.6$) which reflects poor fitting with $Pb^{2+}$, $Co^{2+}$ and methylene blue dye ($0.6 > R^2 > 0.5$) by using faujasite. High fitting of uptake of $Zn^{2+}$ and methylene blue dye ($R^2 > 0.9$) and poorly fitting of uptake $Co^{2+}$, $Cu^{2+}$, $Cd^{2+}$ and $Pb^{2+}$ where correlation coefficient ($R^2 < 0.7$) by using sodalite. The parameters of this model were calculated and listed in Table 5.**

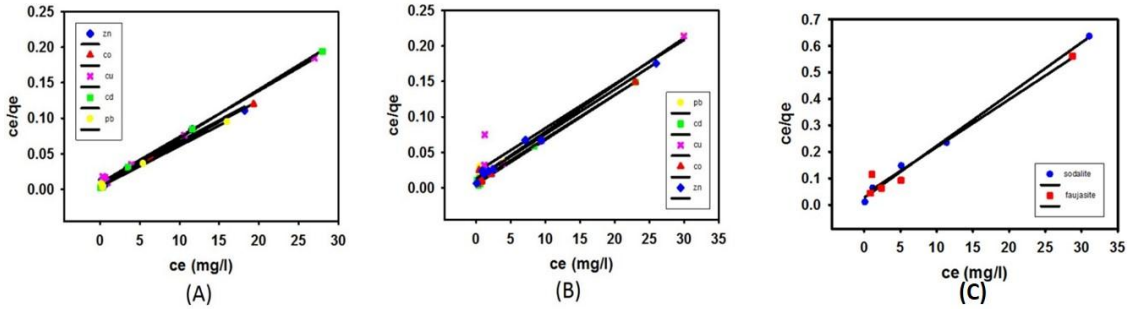


**Fig.14. Langmuir isotherm plot for the adsorption of heavy metals onto faujasite (A) and sodalite (B) and methylene blue dye (C)**

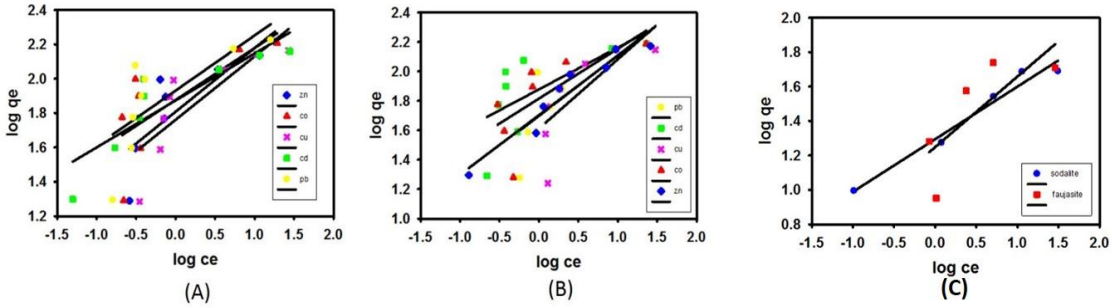


**Fig.15. Freundlich isotherm plot for the adsorption of heavy metals onto faujasite (A) and sodalite (B) and methylene blue dye (C)**
**(Ce = residual concentration of the dissolved heavy metals ions or dye after the adsorption process mg/l)**

**Table 5: Parameters of the studied isothermal models**

| Synthetic minerals | Model | Parameters | $Zn^{2+}$ | $Co^{2+}$ | $Cu^{2+}$ | $Cd^{2+}$ | $Pb^{2+}$ | Methylene blue dye |
|---|---|---|---|---|---|---|---|---|
| Faujasite | Langmuir model | $q_{max}$ (mg/g) | 166.6 | 163.93 | 149.25 | 147.05 | 169.49 | 55.55 |
| | | b (l/mg) | 0.8571 | 1.22 | 0.8375 | 2.266 | 1.966 | 0.473 |
| | | $R^2$ | 0.987 | 0.991 | 0.995 | 0.999 | 0.995 | 0.972 |
| | | $R_L$ | 0.538 - 0.0115 | 0.0757 - 0.008 | 0.1066-0.0117 | 0.0422-0.004 | 0.0484-0.005 | 0.174-0.015 |
| | Freundlich model | l/n | 0.370 | 0.301 | 0.368 | 0.273 | 0.321 | 0.409 |
| | | $K_F$ | 64.12 | 75.16 | 57.67 | 74.64 | 85.11 | 17.70 |
| | | $R^2$ | 0.718 | 0.568 | 0.668 | 0.772 | 0.535 | 0.564 |
| Sodalite | Langmuir model | $q_{max}$ (mg/g) | 149.25 | 156.25 | 144.92 | 156.25 | 144.92 | 52.63 |
| | | b (l/mg) | 0.558 | 0.914 | 0.328 | 1.6 | 0.575 | 0.703 |
| | | $R^2$ | 0.99 | 0.985 | 0.909 | 0.995 | 0.987 | 0.995 |
| | | $R_L$ | 0.151 - 0.017 | 0.098 - 0.010 | 0.233 - 0.029 | 0.058 - 0.0062 | 0.148 - 0.017 | 0.124 - 0.017 |
| | Freundlich model | l/n | 0.403 | 0.338 | 0.471 | 0.283 | 0.410 | 0.305 |
| | | $K_F$ | 50.35 | 65.31 | 40.83 | 75.33 | 49.88 | 19.67 |
| | | $R^2$ | 0.923 | 0.572 | 0.556 | 0.469 | 0.627 | 0.968 |

## 7.1.5. Kinetic models

**Heavy metals uptake was studied by using three kinetic models. The first model Lagergren pseudo–second order kinetic model. This model described the adsorption process as chemosorption which occur through sharing or cation exchange between adsorbent and the dissolved heavy metals (Hui et al, 2005). The linear form of this model was represented in Eq (4):**

$$\frac{t}{q_t} = \frac{1}{k_2 qe^2} + \frac{t}{q_e} \qquad (4)$$

**Where, $q_t$ is the amount of adsorbed heavy metal ions at time t (mg/g) and $K_2$ is the rate constant of pseudo – second order uptake (g/mg min). The linear regression plotting ($t/q_t$) versus (t) for the adsorption of heavy metals ($Pb^{2+}$, $Cd^{2+}$, $Cu^{2+}$, $Co^{2+}$ and $Zn^{2+}$) and organic matter (methylene blue dye) (Fig.16) reflects well fitting of the uptake results with the determination coefficient (more than 0.9). Different parameters using the kinetic models of the heavy metals based on the slope and intercept were calculated and listed in Table 6. The calculated theoretical $q_{e,cal}$ values are 15.62 mg/g, 33.33 mg/g, 35.71 mg/g, 40 mg/g and 40 mg/g for the uptake of $Zn^{2+}$, $Co^{2+}$, $Cu^{2+}$, $Cd^{2+}$, $Pb^{2+}$ and methylene blue dye respectively by using faujasite.**

**While $q_{e,cal}$ values are 37.03 mg/g, 32.25 mg/g, 38.46 mg/g, 37.03 mg/g and 40 mg/g for the uptake of $Zn^{2+}$, $Co^{2+}$, $Cu^{2+}$, $Cd^{2+}$, $Pb^{2+}$, and methylene blue dye respectively by using sodalite. The matching between the estimated experimental uptake equilibrium values and the theoretical calculated ones reflects the fitting of the adsorption results with Lagergren pseudo – second order kinetic model (cf. Seliem et al, 2016).**

**The second model applied herein is the intra-particle kinetic model which deals the transportation of the dissolved ions from the prepared solutions to the synthetic materials followed by intra-particle diffusion/transport process (Demiral and Gündüzoğlu, 2010; Shaban and Abukhadra, 2017). The linear form of the intra-particle diffusion kinetic model was represented in Eq (5):**

$$q_t = Kpt^{\frac{1}{2}} + C \qquad (5)$$

**Where, $K_p$ is the rate constant of the intra-particle diffusion model ($mg/g^{-1}$ $min^{-1/2}$) and C is the intercept which related to the thickness of the boundary layer. Plotting of $q_t$ versus the square root of time was shown in Figure 17. The uptake curves by using both synthetic faujasite and sodalite show more than one adsorption step don't pass through the origin. Thus, the process of uptake of dissolved ions are controlled by more than one uptake mechanism (Katal *et al*., 2012; Seliem *et al*., 2015). The last model Elovich kinetic model which is used herein to describe the second order kinetics if the adsorbent surface is energetically heterogeneous (Wu *et al*., 2009). The linear form of this model was represented in Eq (6):**

$$q_t = \frac{1}{\beta}\ln\ (\alpha\,\beta) + \frac{1}{\beta}\ln(t) \qquad (6)$$

**Where α is the initial adsorption rate (mg/g min) of contact time t = 0 min and β is the extent of surface area coverage and activated energy (g/mg).**

**Plotting of $q_t$ versus ln(t) is shown in Figure 18. The parameters of this model α and β were calculated and presented in Table 6. The results of heavy metals adsorption show high and medium fitting with model ($R^2$ > 0.7, $R^2$ > 0.8, $R^2$ > 0.9) by using faujasite and sodalite. This indicates the energetically heterogenous surface for adsorption of faujasite for $Zn^{2+}$ is higher than the uptake of $Cu^{2+}$, than the uptake of $Cd^{2+}$ than the uptake of $Co^{2+}$ than the uptake of $Pb^{2+}$. In addition, it indicates the energetically heterogeneous of sodalite surface for the adsorption of $Cu^{2+}$ is higher than $Co^{2+}$ than the uptake of $Cd^{2+}$ than the uptake of $Pb^{2+}$ than the uptake of $Zn^{2+}$. The behavior of methylene blue dye using both synthesized faujasite and sodalite show high fitting with model ($R^2$ > 0.9).**

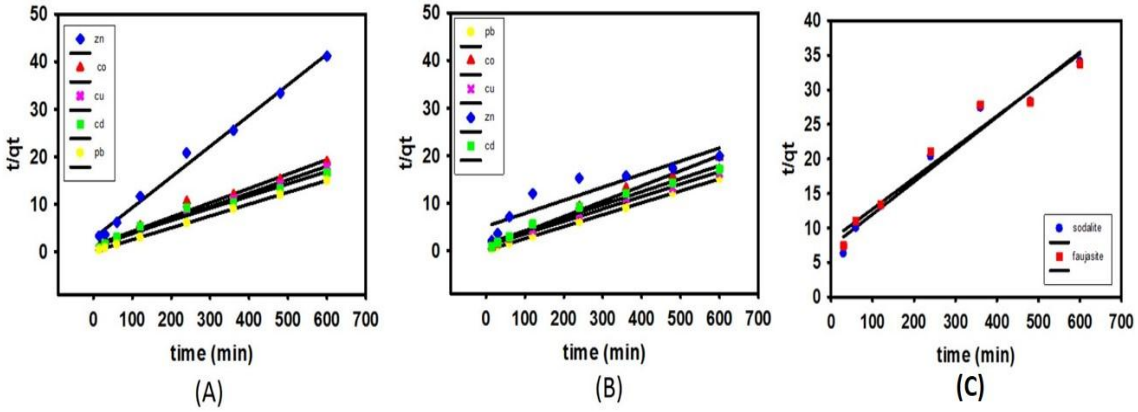


**Fig.16.** **Pseudo-second order kinetic model for the adsorption of heavy metals onto faujasite (A) and sodalite (B) and methylene blue dye (C)**

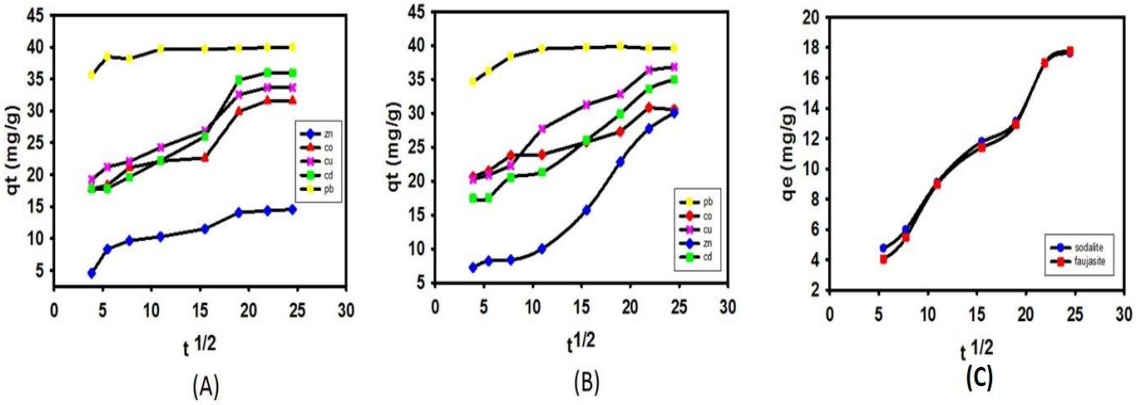


**Fig.17.** **Regression analysis based on intra-particle diffusion model for the adsorption of heavy metals onto faujasite (A) and sodalite (B) and methylene blue dye (C)**

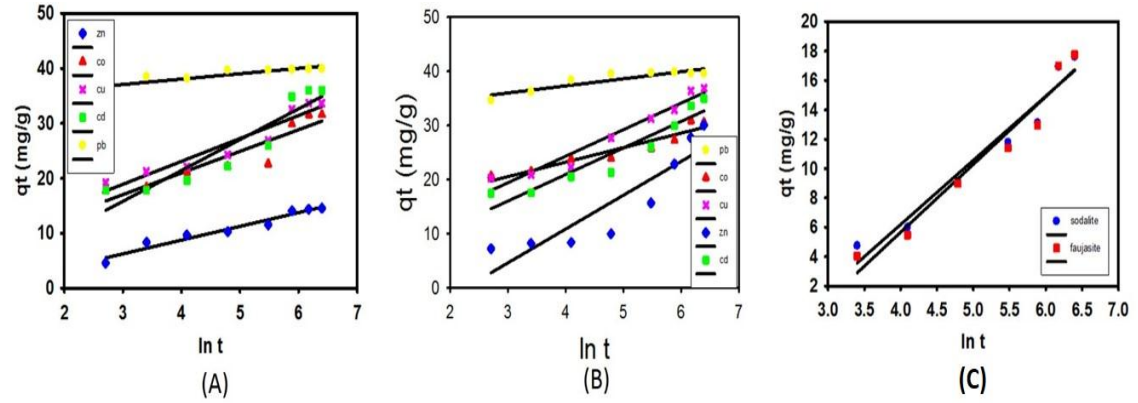


**Fig.18.** **Predictions of the Elovich equation in the adsorption of heavy metals onto faujasite (A) and sodalite (B) and methylene blue dye (C)**

**Table 6: Parameters of kinetic models**

| Synthetic minerals | Model | Parameters | $Zn^{2+}$ | $Co^{2+}$ | $Cu^{2+}$ | $Cd^{2+}$ | $Pb^{2+}$ | Methylene blue dye |
|---|---|---|---|---|---|---|---|---|
| Faujasite | Pseudo – second order | $K_2$ (g/mg min) | $1.4 \times 10^{-3}$ | 7.34 | $0.7 \times 10^{-3}$ | $0.4 \times 10^{-3}$ | $1.3 \times 10^{-3}$ | $0.235 \times 10^{-3}$ |
| | | $q_{e,cal}$ (mg/g) | 15.62 | 33.33 | 35.71 | 40 | 40 | 22.72 |
| | | $R^2$ | 0.993 | 0.980 | 0.991 | 0.978 | 1 | 0.958 |
| | Elovich model | β (mg/g) | 0.4 | 0.25 | 0.23 | 0.17 | 1.02 | 0.216 |
| | | α (mg/g min) | 1.52 | 14.98 | 20.14 | 4.90 | 1.46 | 0.289 |
| | | $R^2$ | 0.952 | 0.859 | 0.918 | 0.869 | 0.777 | 0.953 |
| Sodalite | Pseudo – second order | $K_2$ (g/mg min) | $0.1 \times 10^{-3}$ | $1.1 \times 10^{-3}$ | $0.7 \times 10^{-3}$ | $0.4 \times 10^{-3}$ | $1.5 \times 10^{-3}$ | $0.303 \times 10^{-3}$ |
| | | $q_{e,cal}$ (mg/g) | 37.03 | 32.25 | 38.40 | 37.03 | 40 | 21.27 |
| | | $R^2$ | 0.908 | 0.995 | 0.994 | 0.981 | 1 | 0.963 |
| | Elovich model | B (mg/g) | 0.16 | 0.373 | 0.20 | 0.20 | 0.76 | 0.228 |
| | | α (mg/g min) | 0.65 | 286.45 | 13.12 | 6.57 | $5.63 \times 10^{10}$ | 0.331 |
| | | $R^2$ | 0.818 | 0.902 | 0.953 | 0.897 | 0.826 | 0.953 |

# 8. SUMMARY AND CONCLUSION

**The studied claystones were deposited under variable environmental settings ranging from the continental to open marine environments. Although the investigated samples have different mineralogical composition, nothing has been observed concerning the nature of the synthesized materials. Faujasite and sodalite were synthesized from all the studied samples irrespective of their environmental conditions. Si/Al ratio has no impact on the zeolite mineral type. No claystones of specific sedimentary environment or area needed for the synthesis of zeolites. Therefore, it is not so important to use the kaolin of Sinai or Kalabsha for the synthesis of zeolites. Faujasite and sodalite have revealed enormous removal capacity of heavy metals (Pb, Co, Cu, Cd and Zn) and organic matter (methylene blue dye). The competition between Pb, Zn, Co, Cd and Cu for surface sites onto zeolites was depended primarily on the characteristics of the metal ions and nature of the substrate (crystallinity, morphology and surface area). The maximum uptake of heavy metals reaches up to 99.9%, while the organic matter reaches up to 75.05%. Faujasite and sodalite behave similarly concerning the removal of Pb, they have the ability to remove it at lower experimental condition (pH 4, time 120 min). Faujasite has the capacity to remove Cd, Cu, Zn and Co at lower condition also (pH 4,5, time 120, 360 min). Sodalite, in contrast, required higher experimental conditions for the removal of Cd, Cu, Zn and Co, it removes these metals at pH 4, 7 and time 120, 480 min. A marked**

**variation in the uptake of organic matter between faujasite and sodalite was noticed. The former removes about 75.05%, while Sodalite removes 46.7%. The adsorption pseudo – second order isothermal and kinetic models data fitted well the Langmuir and Freundlich.**

## ACKNOWLEDGMENT:

**I would like to sincerely express my appreciation to my supervisors Prof. Ezzat A. Ahmed and Prof. Mamdouh F. Soliman for their valuable supports, encouragement, discussions and prompt help during the preparation of this article.**

## REFERENCES

**Abudaia, A. J., Sulyman, O. M., Elazaby, Y. K., Ben-Ali, M. S. (2013) Adsorption of Pb (II) and Cu (II) from Aqueous Solution onto Activated Carbon Prepared from Dates Stones. International Journal of Environmental Science and Development, Vol. 4, No. 2.**

**Allen, S. J., Gan, Q, Matthews, R, Johnson, P.A. (2003) Comparison of optimized isotherm models for basic dye adsorption by kudzu. Bioresour. Technol. 88: 143-152.**

**Bagherifam, S., Komarneni, S., Lakzian, A., Fotovat, A., Khorasani, R., Huang, W., Ma, J., Hong, S., Cannon, F.S, Wang, Y. (2014) Highly selective removal of nitrate and perchlorate by organoclay. Appl. Clay Sci 95 :126-132.**

**Barrer, R. M. (1938) The sorption of polar and non-polar gases on zeolites. Proceedings of the Royal Society of London 167A: 392-419.**

**Chowdhury, H. and Naskar, M. K. (2016) Hexagonal sheet-like mesoporous titanium phosphate for highly efficient removal of lead ion from water. RSC Adv. 6, 67136–67142.**

**Cronstedt, A. F. (1756) Ron och beskriting om en obekant bärg ant, som kallas zeolites. Akad. Handl. Stockholm, 18, 120 – 130.**

**Demiral, H. and Gündüzoğlu, G. (2010) Removal of nitrate from aqueous solutions by activated carbon prepared from sugar beet bagasse. Bioresour. Technol 101:1675-1680.**

**Deville, C. H. (1862) Comptes Rendus Acad. Sci., 54, 324.**

**Flanigen, E. M. (2001) Zeolites and molecular sieves. An historical perspective, in Introduction to Zeolite Science and Practice, 2nd ed (eds H. Van Bekkum, E.M. Flanigen, P.A. Jacobs, and J.C. Jensen), Stud. Surf. Sci. Catal., vol. 137, Elsevier, Amsterdam, pp. 11 – 35.**

**Golbad, S. (2016) Synthesis and Characterization of Microporous and Mesoporous Zeolites from Fly ash for Heavy Metal Removal from Wastewater. Master of Science in Engineering. University of Wisconsin- Milwaukee. 94p.**

**Hafiza, N., Razak, A., Praveena, S. M., Hashim, Z., Zaharin, A. (2015) Drinking water studies: a review on heavy metal, application of biomarker and health risk assessment. J. Epidemiol. Glob. Health 5, 297–310.**

**Henderson, C.M.B. and Taylor, D. (1977) Infrared spectra of anhydrous members of the sodalite family. Spectrochim Acta, Vol. 33A, pp.283 to 290.**

**Hui, K. S., Chao, C.Y.H., Kot, S. C. (2005) Removal of mixed heavy metal ions in wastewater by zeolite 4A and residual products from recycled coal fly ash. Journal of Hazardous Materials B127:89–101.**

**Hums, E. (2017) Synthesis of Phase-Pure Zeolite Sodalite from Clear Solution Extracted from Coal Fly Ash. J Thermodyn Catal, Volume 8. Issue 2. 1000187.**

**Joshi, U. D., Joshi P. N., Tamhankar S. S., Joshi V. V., Rode C. V., Shiralkar V. P. (2003) Effect of nonframework cations and crystallinity on the basicity of Na x zeolites. Appl. Catal. A; 239: 209-220.**

**Katal, R. M. S., Baei M. S., Rahmati H. T., Esfandian, H. (2012) Kinetic, isotherm and thermodynamic study of nitrate adsorption from aqueous solution using modified rice husk. J. Ind. Eng. Chem 18: 295-302.**

**Khalil, S. and McClay, K. (2002) Extensional Fault-Related Folding, Northwestern Red Sea, Egypt. Journal of Structural Geology, Vol. 24, No. 4, pp. 743-762.**

**Lian, L., Li ping G., Guo, C. (2009) Adsorption of Congo red from aqueous solutions onto Ca-bentonite. J. Hazard. Mater 161 (1):126–131.**

**Ltaief, O., Siffert, S., Fourmentin, S., Benzina, M. (2015) Synthesis of Faujasite type zeolite from low grade Tunisian clay for the removal of heavy metals from aqueous waste by batch process: Kinetic and equilibrium study. Acade´mie des sciences. C. R. Chimie xxx (2015) xxx–xxx. Published by Elsevier. 11 p.**

**Manohar, S., Jadia, C. D., Fulekar, M. H. (2006) Impact of ganesh idol immersion on water quality. Indian J. Environ. Prot. 27(3), 216-220.**

**Mozgawa, W. (2001) The relation between structure and vibrational spectra of natural zeolites. J. Mol. Struct.; 596:129–137.**

**Novembre, D., DiSabatino, B., Gimeno, D., Garcia-Valle`s, M., Manent, S. (2004) Synthesis of Na-X zeolites from tripolaceous deposits (Crotone, Italy) and volcanic zeolitized rocks (Vico Volcano, Italy). Microporous and Mesoporous Materials, 75, 1-11.**

**Polatoglu, I. (2005) Chemical Behavior of Clinoptilolite rich natural Zeolite in Aqueous Medium. Master thesis, Graduate School of Engineering and Sciences of Izmir Institute of Technology, Turkey, ١٥٤p.**

**Rhaiti, H., Laghzizil, A., Saoiabi A., El Asri, S., Lahlil, K., Gacoin, T. (2012) Surface properties of porous hydroxyapatite derived from natural phosphate. Materials Chemistry and Physics 136,1022-1026.**

**Ríos, C. A., Williams, C.D., Fullen, M. A. (2009) Nucleation and Growth History of Zeolite LTA Synthesized from Kaolinite by Two Different Methods. *Applied Clay Science*, 42, 446-454.**

**Said, R. (1990). The Geology of Egypt. Balkema, Rotterdam, Brookfield, 734p.**

**Seliem, M. K., Mohamed, E.A., Selim, A.Q., Shahien, M. G., Abukhadra, M. R. (2015) Synthesis of Na-A Zeolites from Natural and Thermally Activated Egyptian Kaolinite: Characterization and Competitive Adsorption of Copper Ions from Aqueous Solutions. International Journal of Bioassays 4:4423–4430.**

**Seliem, M. K., Komarneni, S., AbuKhadra, M. R. (2016) Phosphate removal from solution by composite of MCM-41 silica with rice husk: kinetic and equilibrium studies. Microporous and Mesoporous Materials J 224: 51–57.**

**Sen, T. K. and Gomez. D. (2011) Adsorption of zinc ($Zn^{2+}$) from aqueous solution on natural bentonite. Desalination. 267(2), 286-294.**

**Shaban, M., Abukhadra, M. R., Shahien M. G., Suzan S. I. (2017) Novel bentonite/zeolite NaP composite efficiently removes methylene blue and Congo red dyes. Environ Chem Lett. DOI 10.1007/s10311-017-0658-7.**

**Shaban, M. and Abukhadra, M. R. (2017) Geochemical evaluation and environmental application of Yemeni natural zeolite as sorbent for $Cd^{2+}$ from solution: kinetic modeling, equilibrium studies, and statistical optimization. Environ Earth Sci. 76:310. DOI 10.1007/s12665-017-6636-3.**

**Thuadaija, P. and Nuntiya, A. (2012) Preparation and Characterization of Faujasite using Fly Ash and Amorphous Silica from Rice Husk Ash. Procedia Engineering. Published by Elsevier Ltd. 32: 1026 – 1032.**

**Wu, F. C., Tseng, R. L., Juang, R. S. (2009) Characteristics of Elovich equation used for the analysis of adsorption kinetics in dye-chitosan systems. Chemical Engineering Journal 150: 366–373.**

# إستغلال الصخور الطينية بمنطقة القصير، البحر الأحمر، مصر، في تخليق معادن الزيوليت وإستخدامها في معالجة المياه

**فاطمه درديز**

**قسم الجيولوجيا ، كلية العلوم، جامعة أسيوط**

**الملخص :**

**يهدف هذا البحث أساساً إلي تقييم الصخور الطينية للكريتاوي العلوي – الباليوجين المبكر والمترسبة في بيئات نهرية، مد وجزر بالإضافة إلي بيئات بحرية مفتوحة في تخليق معادن الزيوليت وقد دلت دراسة حيود الأشعة السينية علي أن الصخور الطينية مجال الدراسة تتكون أساساً من الكوارتز ،الإسمكتيت ،الكاولينيت والكالسيت. وبمعالجة هذه الصخور باستخدام هيدروكسيد الصوديوم عند درجة حراره ٨٠o، ١٦٠o أدت إلي تكوين معدني الفيجوسيت والصودالايت علي الترتيب وتم التأكد من ذلك باستخدام حيود الأشعة السينية ،الميكروسكوب الإلكتروني الماسح ،الأشعة تحت الحمراء وإمتصاص النيتروجين.**

**ودلت الدراسة علي أن معدني الفيجوسيت والصودالايت لهم قدرة مذهلة في إزالة المادة العضوية بالإضافة إلي عناصر الكوبلت ،الرصاص ،الكادميوم ،الزنك والنحاس من المياه الملوثة وعامةً فإن هذه المعادن لها قدرة أكبر في إزالة العناصر الثقيلة مقارنةً بالمادة العضوية حيث تصل نسبة إزالة المعادن الثقيلة إلي حوالي ٩٩.٩% في حين أن إزالة المادة العضوية تصل إلي ٧٥.٥% أضف إلي ذلك لا يوجد تغير معنوي بين معدني الفيجوسيت والصودالايت لإمتصاص العناصر الثقيلة أو المادة العضوية.**